



OPEN

## Analysis of associated factors affecting hematoma evacuation rates in spontaneous intracerebral hemorrhage with stereotactic aspiration combined with catheter drainage

Xinqun Luo<sup>1,2,5</sup>, Keming Song<sup>3,5</sup>, Lingyun Zhuo<sup>1,5</sup>, Fuxin Lin<sup>1,2</sup>, Zhuyu Gao<sup>1,2</sup>, Qiu He<sup>1,2</sup>, Yan Zheng<sup>1,2</sup>, Kunbin Lian<sup>1,2</sup>, Huangcheng Shangguan<sup>1,2</sup>, Xingguang Luo<sup>4</sup>, Yuanxiang Lin<sup>1,2</sup>, Dezhi Kang<sup>1,2</sup>✉ & Wenhua Fang<sup>1,2</sup>✉

Due to the absence of direct visualization during the operative field in stereotactic surgery for sICH, there exists individual variability in hematoma evacuation (HE) rates, with about 42% of patients not attaining the expected threshold for HE. The aim of this study was to find the relevant factors affecting HE during the treatment of sICH with stereotactic surgery. We pooled individual data from our prospective ICH database, encompassing patients who underwent stereotactic aspiration and catheter drainage. The primary outcome was HE rates prior to extubation. Multivariate logistic regression using the stepwise forward method to identify the independent risk factors. A predictive scoring model was developed based on regression coefficients. To evaluate its discrimination performance, we conducted ROC curve analysis and calculated the AUC. Additionally, we employed calibration curves as an indicator of concordance. The bootstrap internal validation was used to ascertain the model's stability. DCA was performed to determine the clinical utility. The study included 90 patients, of whom 43 (47.8%) patients achieved HE rates  $\geq 70\%$ . The multivariate logistic analysis showed that blend sign (OR 7.003, 95% CI 2.118–23.161,  $P = 0.001$ ), irregular shape (OR 0.235, 95% CI 0.067–0.821,  $P = 0.023$ ), two drainage tubes (OR 28.643, 95% CI 1.872–438.181,  $P = 0.016$ ), diabetes (OR 0.078, 95% CI 0.006–0.948,  $P = 0.045$ ), and hematoma edge linked to ventricle (OR 0.145, 95% CI 0.032–0.659,  $P = 0.012$ ) were independent risk factors. For clinical use, the Model-score was established, with a total score ranging from -6 to 5. The AUC values of the Model-logit and Model-score were 0.820 (95% CI 0.733–0.906) and 0.822 (95% CI 0.737–0.908) respectively. The cutoff values were 0.275 and -0.5. Calibration curves demonstrated excellent agreement between predicted probabilities and observed outcomes in both models. Utilizing the bootstrap method for internal validation, the mean AUC values were determined to be 0.819 (95% CI 0.736–0.903) for Model-logit and 0.823 (95% CI 0.742–0.903) for Model-score, demonstrating stability across the resampled datasets. The DCA confirmed that both models provide superior net benefit for predicting HE rates  $\geq 70\%$  when the individualized threshold ranges from 10 to 82%. The predictive model of HE rates  $\geq 70\%$  prior to extubation has demonstrated predictive capability, holds the potential to assist clinicians in optimizing surgical efficiency.

**Keywords** Blend sign, Hematoma evacuation rates, Predictive model, Spontaneous intracerebral hemorrhage, Stereotactic aspiration

### Abbreviations

AUC	Area under the curve
CT	Computed tomography
CI	Confidence interval
DCA	Decision curve analysis
DICOM	Digital Imaging and Communications in Medicine

GCS	Glasgow coma scale
HE	Hematoma evacuation
HU	Hounsfield unit
mRS	Modified Rankin Scale
NCCT	Non-contrast computed tomography
OR	Odds ratio
ROC	Receiver operating characteristic
ROI	Region of interest
sICH	Spontaneous intracerebral hemorrhage

<sup>1</sup>Department of Neurosurgery, Neurosurgery Research Institute, The First Affiliated Hospital, Fujian Medical University, No. 20 Chazhong Road, Taijiang District, Fuzhou 350005, Fujian, China. <sup>2</sup>Department of Neurosurgery, National Regional Medical Center, Binhai Campus of the First Affiliated Hospital, Fujian Medical University, Fuzhou 350212, Fujian, China. <sup>3</sup>Department of Neurosurgery, Shunchang County General Hospital, Nanping 353200, Fujian, China. <sup>4</sup>Beijing Huilongguan Hospital, Peking University Huilongguan School of Clinical Medicine, Beijing 100096, China. <sup>5</sup>Xinqun Luo, Keming Song and Lingyun Zhuo contributed equally to this work and share first authorship. ✉email: kdz99988@vip.sina.com; fang.wenhua@qq.com

Spontaneous intracerebral hemorrhage (sICH), one of the most severe stroke subtypes, is associated with high global morbidity and mortality, ranking as the second leading cause of death worldwide<sup>1–4</sup>. The underlying pathological mechanism primarily involves nontraumatic rupture of intracranial arteries, veins, or capillaries. Subsequent extravasation of blood into brain parenchyma induces mass effects and secondary tissue damage mediated by erythrocyte lysis<sup>5–8</sup>. The treatment of sICH is still controversial<sup>9,10</sup>. Theoretically, removing as much of the hematoma as possible can halt the adverse effects arising from it. In recent years, with the continuous development of surgical treatment of sICH, minimally invasive surgery combined with catheter drainage has been proved to be safe and effective<sup>11,12</sup>, which is the promising method in treating sICH. The MISTIE III trial showed that if the residual volume of hematoma is controlled within 15 mL or the evacuation rates of hematoma are more than 70%, it is promising to improve the neurological status one year after operation<sup>11,13</sup>. Compared with traditional craniotomy, stereotactic surgery demonstrates distinct clinical advantages: lower intraoperative blood loss, reduced tissue trauma, faster neurological recovery, and shorter hospitalization duration. Furthermore, its cost-effectiveness significantly alleviates the financial burden on both patients and healthcare systems, making it particularly suitable for implementation in resource-limited healthcare settings<sup>14–16</sup>. Hematoma volume represents the most critical prognostic indicator in sICH patients<sup>17,18</sup>. Nevertheless, stereotactic surgery faces inherent limitations: due to blood clot coagulation and the absence of direct intraoperative visualization impair surgical efficiency, often necessitating staged interventions for partial hematoma removal. These constraints underscore the imperative to optimize hematoma evacuation (HE) rates in stereotactic aspiration and catheter drainage protocols, which holds profound clinical relevance for mitigating secondary injury pathways.

However, there are still few studies focusing on the factors affecting the evacuation rates of intracerebral hematoma after stereotactic surgery. Therefore, this study evaluated the clinical and imaging characteristics of sICH patients who underwent stereotactic aspiration and catheter drainage from a prospective collected, multicenter intracerebral hemorrhage database and analyzed the factors affecting the evacuation rates of hematoma.

## Methods

### Patients

We recruited sICH patients from our prospectively maintained sICH patient database (Risa-MIS-ICH, ClinicalTrials.gov Identifier: NCT03862729) between July 2019 and July 2023. The criteria for inclusion are as follows: (1) Supratentorial cerebral parenchymal hemorrhage was diagnosed by computed tomography (CT) before surgery, and complete CT image data were available for postoperative follow-up; (2) Patients underwent stereotactic hematoma aspiration and catheter drainage; (3) There are no metal artifacts on CT image, which can accurately calculate the volume of hematoma. The exclusion criteria: (1) Conservative treatment or any other surgical intervention (such as endoscopic hematoma resection, craniotomy hematoma removal, or only external ventricular drainage, etc.); (2) Infratentorial cerebral hemorrhage, specifically in the cerebellum or brainstem; (3) The inadequate quality of postoperative follow-up CT imaging, which impeded accurate assessment; (4) Loss of CT data; (5) For patients who initially underwent stereotactic surgery but subsequently required other surgical interventions (such as endoscopic surgery, craniotomy, etc.) due to disease progression, they were also excluded from the study. The surgical operations were executed with precision, adhering strictly to standardized protocols. While the stereotactic equipment may vary among different medical centers due to disparities in resources, the fundamental approach remains consistent: minimally invasive hematoma puncture aspiration and catheter placement for drainage. A postoperative CT scan was performed within 24 h to ascertain the catheter placement. In order to prevent retrograde infection, the drainage tube is usually left in place for 3 to 5 days. All related treatments adhere to the guideline of the American Heart Association / American Stroke Association (AHA/ASA) for the management of sICH<sup>9</sup>. Prior to their involvement, all participants or their legal representatives provided written informed consent. This study was approved by the Ethics Committee of the First Affiliated Hospital of Fujian Medical University (Ethical Approval Number: MRCTA, ECFAH of FMU [2018] 082-1) and complied with relevant laws and regulations.

## Data collection

Initial and follow-up CT image data for all patients were archived in the Digital Imaging and Communications in Medicine (DICOM) format. The hematoma was detected layer by layer on the axial section through 3D slicer (version No. 5.2.2), and the threshold value of hematoma was set between 44 and 100 Hounsfield unit (HU)<sup>19</sup>. The specific value could fluctuate depending on the actual situation; the upper limit should not exceed 100 HU, and the lower limit should not be lower than 35 HU. The region of interest (ROI) was delineated, and the volume and CT value of hematoma were calculated by automatic segmentation. The 3D slicer can automatically calculate the mean CT value of the entire hematoma, indirectly reflecting the density of the entire hematoma. The primary endpoint of this study aimed to evaluate the HE rates prior to extubation following stereotactic aspiration and catheter drainage. The calculation of HE rates was determined as follows:

$$\text{HE rates} = [(\text{Hematoma volume recorded within 6 h before surgery}) - (\text{Hematoma volume measured prior to extubation})] / (\text{Hematoma volume within the 6 h prior to surgery}).$$

Based on the subgroup analysis results from the MISTIE trial<sup>11</sup>, we classified hematoma evacuation as “good” when HE rates  $\geq 70\%$ , and “poor” when HE rates  $< 70\%$ .

General information of patients was extracted from the database, such as gender, age, current or previous smoking and drinking, history of diabetes and hypertension, medication history (such as anticoagulant drugs, antiplatelet drugs), GCS score at admission, duration of hospitalization, total hospitalization expenses. In addition, surgery-related information was collected, such as the number of drainage tubes, use of urokinase, and duration of catheter placement. Functional status at discharge and prognosis during the 3 to 12 months follow-up period were evaluated using the modified Rankin Scale (mRS). The mRS score of 0 to 3 was defined as favorable functional outcomes.

Baseline non-contrast CT (NCCT) markers were examined by two independent investigators (XQ L, KB L) in all patients. The researchers did not know the patients' clinical history and follow-up CT results. The detected NCCT markers and their definitions are as follows: (1) Black hole sign: a relatively hypoattenuating area encapsulated with a hyperattenuating hematoma. The boundary is clear, and there is a density difference of at least 28 HU between the two regions. The low-density area can be round, oval, or strip but should not be connected to the adjacent brain tissue<sup>20</sup>; (2) Island sign: at the same level, there are  $\geq 3$  scattered small hematoma separated from the main hematoma, or  $\geq 4$  small hematomas, some or all of which are connected to the main hematoma<sup>21</sup>; (3) Satellite sign: there is a high-density small hematoma separated from the main hematoma on at least one level. The maximum diameter of the small hematoma is less than 10mm, the maximum distance between the small hematoma and the main hematoma is less than 20mm, and intraventricular involvement or subarachnoid extension of the main hematoma are excluded<sup>22</sup>; (4) Blend sign: a relatively high-density area next to a low-density area of the hematoma. The boundary between the two regions is well-defined and can be identified by the naked eye, and the CT value difference is more than 18HU. The hypoattenuating area is not surrounded by the hyperattenuating area<sup>23</sup>; (5) Fluid level: there is at least one distinct ICH region with a low CT attenuation region above (hypodense compared to brain) and a high CT attenuation region below (hyperdense compared to brain), separated by a clear horizontal line<sup>24</sup>. Irregular hematoma morphology is defined by the Barras shape scale as two or more irregular shapes on the margins of the hematoma, which is assessed on the axial slice<sup>25</sup>. The definition of the hematoma edge linked to the ventricle is that the parenchymal hematoma breaks into the ventricle, and the hematoma edge is tangent to the ventricle. Other definitions include deep hematoma: hematoma greater than 1cm from the cortex<sup>26</sup>; Postoperative hematoma expansion: reexamination within 24 h find an augmentation of 6 ml or a 33% expansion relative to its preoperative dimensions<sup>27</sup>. Based on previous experience, we employed the following catheter position scoring: a score of 3 for lateral catheter holes positioned precisely at the center of the hematoma, a score of 2 for those located within the cavity of the hematoma but outside the center, a score of 1 for holes situated at the hematoma's edge, and a score of 0 for those positioned completely outside the hematoma, signifying an inadequate location<sup>28,29</sup>. Discrepancies about the occurrence of CT markers were settled by joint discussion of the two researchers.

## Statistical analysis

Statistical analysis was performed using IBM SPSS Statistics (Version 27.0, SPSS Inc., Chicago, USA) and R language (Version 4.4.1, Institute for Statistics and Mathematics, Vienna, Austria). The graphical were created using GraphPad Prism version 9 (GraphPad Software, San Diego, CA, USA). Continuous variables consistent with normal distribution were presented as mean  $\pm$  standard deviations (SD), while those consistent with non-normal distribution were presented as median interquartile range (IQR). Categorical variables were expressed as frequencies (percentages). The demographic characteristics, clinical data, and CT markers between patients with and without HE rates  $\geq 70\%$  were compared using the Pearson chi-square test, Fisher exact test, Student's t-test, or the Mann–Whitney U test as appropriate. Multivariate logistic regression using the stepwise forward method to identify the independent risk factors. A logistic model (Model-logit) was established based on the independent risk factors. For clinical use, we assigned points for each of the factors based on the regression coefficients and developed a new model (Model-score). Receiver operating characteristic (ROC) curves were generated to calculate the area under the curve (AUC) and cutoff value. The discriminatory ability of the model was assessed using the AUC with 95% confidence intervals (CI). The maximal Youden index was used to determine the “optimal” cut-point of the model. The calibration of the model was evaluated with Hosmer–Lemeshow goodness-of-fit test. We did an internal validation using a bootstrap resampling process (1000 times) to provide an estimate of model performance. Finally, decision curve analysis (DCA) was performed to determine the clinical utility by estimating the net benefit at various threshold levels.  $P < 0.05$  was considered statistically significant.

## Result

### Baseline characteristics

The process of patient selection was shown in Fig. 1. Finally, 90 patients with sICH across 10 medical centers were included in this analysis. Of these, 43 patients achieved HE rates  $\geq 70\%$ . In the HE rates  $\geq 70\%$  group, included 37 males (86.0%), the mean age was  $57.23 \pm 16.01$  years. In the HE rates  $< 70\%$  group, included 37 males (78.7%), the mean age was  $57.94 \pm 13.68$  years. Demographics are displayed in Table 1. In the HE rates  $\geq 70\%$  group, a lower incidence of diabetes (4.7% vs 19.1%,  $P=0.036$ ) and postoperative hematoma expansion (2.3% vs 14.9%,  $P=0.036$ ) were observed. Significant statistical differences were found between two groups in terms of blend sign (48.8% vs 21.3%,  $P=0.006$ ), irregular shapes (18.6% vs 42.6%,  $P=0.014$ ), intraventricular hemorrhage (27.9% vs 59.6%,  $P=0.003$ ) and hematoma edge linked to ventricle (9.3% vs 36.2%,  $P=0.003$ ). The median interval from onset to stereotactic surgery was 1 (1–2) days. The preoperative CT showed that 57 patients (63.3%) had deep sICH. The preoperative median hematoma volume of HE rates  $\geq 70\%$  group were 39.20 (32.84–54.36) mL, and the median CT value were 59.65 (56.51–64.64) HU, while those of HE rates  $< 70\%$  group were 38.70 (31.22–54.79) mL and 61.27 (59.94–64.00) HU, respectively. Based on catheter position scoring, we observed 42 (46.7%) patients scoring 3, 22 (24.4%) scoring 2, and 24 (26.7%) scoring 1, only 2 (2.2%) patients exhibited unsatisfactory catheter positioning, necessitating readjustment. Totally, 73 (81.1%) patients received urokinase for thrombolysis, but there was no disparity in HE rates (Table 1). Detailed dosage information for urokinase was provided in Supplementary Table S1.

### Hospitalization and follow-up outcomes

The high-evacuation cohort (HE  $\geq 70\%$ ) demonstrated a significantly shorter median intubation time compared to the low-evacuation group (HE  $< 70\%$ ) (3 days vs 5 days,  $P=0.004$ ), alongside markedly reduced median residual hematoma volume (6.96 mL vs 18.86 mL,  $P<0.001$ ). Despite these procedural advantages, no statistically significant differences were detected between the two groups in discharge neurological status (median GCS: 14.5 vs 13.0,  $P=0.078$ ), functional recovery (mRS scores at discharge and follow-up,  $P>0.05$ ), mortality rates (20.0% vs 23.7%,  $P>0.05$ ), or healthcare resource utilization metrics, including median hospitalization duration (17.0 days vs 17.5 days,  $P=0.383$ ) and total costs (37,200.17 ¥ vs 53,535.32 ¥,  $P=0.145$ ) (Table 2).

### Model-logit and model-score

Using the stepwise forward method, the multivariate logistic regression results are displayed in Table 3. The blend sign [odds ratio (OR) = 7.003, 95% CI 2.118–23.161,  $P=0.001$ ], irregular shape (OR 0.235, 95% CI 0.067–0.821,  $P=0.023$ ), two drainage tubes (OR 28.643, 95% CI 1.872–438.181,  $P=0.016$ ), diabetes (OR 0.078, 95% CI

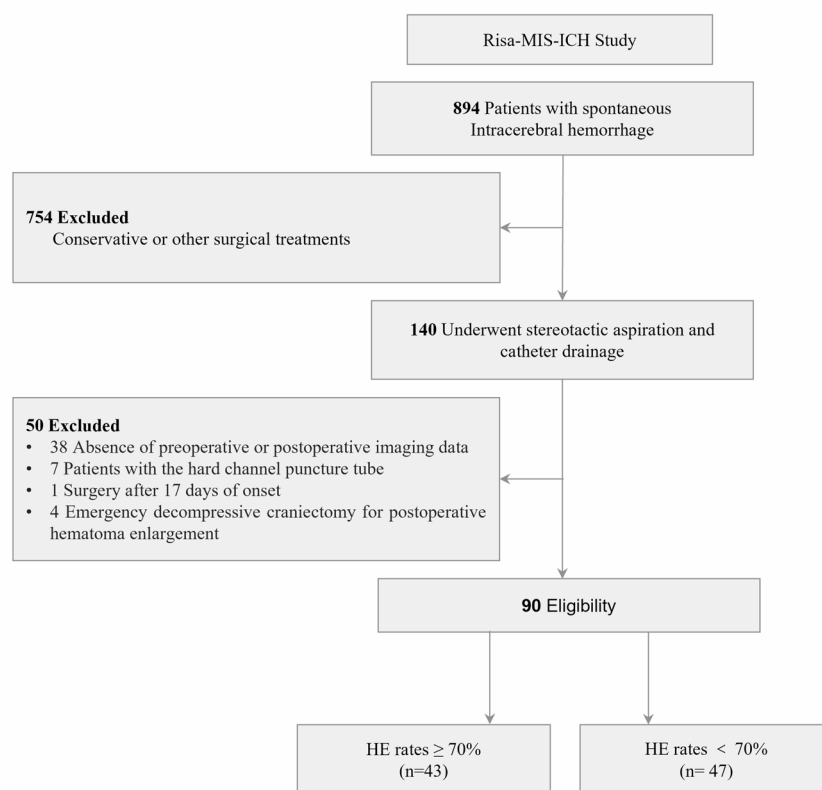


**Fig. 1.** The flow chart of patient selection. HE, hematoma evacuation.

Variables	HE rates $\geq 70\%$ (n = 43)	HE rates $< 70\%$ (n = 47)	Total (n = 90)	P value
Age, years, mean $\pm$ SD	57.23 $\pm$ 16.01	57.94 $\pm$ 13.68	57.60 $\pm$ 14.76	0.823
Male, n (%)	37 (86.0)	37 (78.7)	74 (82.2)	0.364
Smoking, n (%)	9 (20.9)	12 (26.1)	21 (23.6)	0.567
Drinking, n (%)	7 (16.3)	11 (23.9)	18 (20.2)	0.370
Medical history, n (%)				
Diabetes	2 (4.7)	9 (19.1)	11 (12.2)	<b>0.036</b>
Hypertension	28 (65.1)	30 (63.8)	58 (64.4)	0.899
Medication history, n (%)				
Anticoagulation therapy	0	1 (2.1)	1 (1.1)	0.336
Antiplatelet therapy	2 (4.7)	3 (6.4)	5 (5.6)	0.720
Admission GCS scores, median (IQR)	10 (8–14)	11 (9–14)	11 (8.75–14)	0.932
The time from onset to operation, days, median (IQR)	1 (1–3)	1 (1–2)	1 (1–2)	0.063
Radiographic parameters				
Hematoma location, n (%)				0.737
Deep	28 (65.1)	29 (61.7)	57 (63.3)	
Lobe	15 (34.9)	18 (38.3)	33 (36.7)	
Pre-op hematoma volume, mL, median (IQR)	39.20 (32.84–54.36)	38.70 (31.22–54.79)	39.18 (31.96–54.47)	0.544
Pre-op mean hematoma CT value, HU, median (IQR)	59.65 (56.51–64.64)	61.27 (59.94–64.00)	61.18 (58.43–64.08)	0.177
Preoperative CT signs, n (%)				
Black hole sign	15 (34.9)	19 (40.4)	34 (37.8)	0.588
Island sign	10 (23.3)	11 (23.4)	21 (23.3)	0.987
Satellite sign	9 (20.9%)	14 (29.8)	23 (25.6)	0.336
Blend sign	21 (48.8%)	10 (21.3)	31 (34.4)	<b>0.006</b>
Fluid level	3 (7.0)	1 (2.1)	4 (4.4)	0.265
Irregular	8 (18.6)	20 (42.6)	28 (31.1)	<b>0.014</b>
Intraventricular hemorrhage	12 (27.9)	28 (59.6)	40 (44.4)	<b>0.003</b>
Hematoma edge linked to ventricle	4 (9.3)	17 (36.2)	21 (23.3)	<b>0.003</b>
Catheter position score, n (%)				0.518
0	0	2 (4.3)	2 (2.2)	
1	11 (25.6)	13 (27.7)	24 (26.7)	
2	10 (23.3)	12 (25.5)	22 (24.4)	
3	22 (51.2)	20 (42.6)	42 (46.7)	
Catheter parallel hematoma long axis, n (%)	24 (55.8)	23 (48.9)	47 (52.2)	0.514
Two drainage tubes, n (%)	5 (11.6%)	1 (2.1%)	6 (6.7)	0.071
Post-op hematoma expansion, n (%)	1 (2.3)	7 (14.9)	8 (8.9)	<b>0.036</b>
Urokinase, n (%)	34 (81.0)	39 (83.0)	73 (81.1)	0.804

**Table 1.** Comparison of demographic, clinical, and radiological characteristics between patients with and without HE rates  $\geq 70\%$  prior to extubation. CT, computed tomography; GCS, Glasgow Coma Scale; HE, hematoma evacuation; HU, Hounsfield unit; IQR, interquartile range; Pre-op, preoperative; Post-op, postoperative; SD, standard deviation. Variables showing statistical significance ( $P < 0.05$ ) are in bold.

0.006–0.948,  $P = 0.045$ ), and hematoma edge linked to ventricle (OR 0.145, 95% CI 0.032–0.659,  $P = 0.012$ ) were independent risk factors. The distribution range of different hematoma evacuation rates based on these factors were shown in Supplementary Figure S1. Based on these factors, we established the Model-logit and Model-score. The Model-logit was as follows:

$$\text{Logit}(P) = 2.567 + 1.946 * \text{Blend sign (yes = 1, no = 0)} - 1.447 * \text{Irregular shape (yes = 1, no = 0)} + 3.355 * \text{Two drainage tubes (yes = 1, no = 0)} - 2.553 * \text{Diabetes (yes = 1, no = 0)} - 1.931 * \text{Hematoma edge linked to ventricle (yes = 1, no = 0)}.$$

We established Model-score based on the regression coefficients, where each factor was scored by rounding the regression coefficient to the nearest value, with a total score ranged from -6 to 5 (Table 3). To evaluate the models' discrimination performance, we generated ROC curve. Notably, the AUC values for Model-logit and Model-score were 0.820 (95% CI 0.733–0.906) and 0.822 (95% CI 0.737–0.908), respectively (Fig. 2). Based on the highest Youden index, the cutoff values were 0.275 and -0.5, respectively. The sensitivity and specificity were 97.7% and 53.3% for Model-logit, and 95.3% and 55.3% for Model-score (Supplementary Table S2, Table S3). Both models displayed a relatively robust predictive performance. We considered that patients with scores of -6



Variables	HE rates $\geq 70\%$ (n = 43)	HE rates $< 70\%$ (n = 47)	Total (n = 90)	P value
Intubation time, days, median (IQR)	3 (1–4)	5 (3–7)	4 (2–5)	0.004
Residual hematoma volume, mL, median (IQR)	6.96 (3.52–9.97)	18.86 (15.74–30.80)	13.43 (6.63–20.11)	$< 0.001$
mRS score at discharge, n (%)				0.844
0–3	8 (18.6)	8 (17.0)	16 (17.8)	
4–6	35 (81.4)	39 (83.0)	74 (82.2)	
Discharge GCS scores, median (IQR)	14.5 (11–15)	13 (7–15)	13 (10–15)	0.078
mRS score at last follow-up, n (%) a				0.699
0–3	20 (57.1)	20 (52.6)	40 (54.8)	
4–6	15 (42.9)	18 (47.4)	33 (45.2)	
Mortality at last follow-up, n (%) a	7 (20.0)	9 (23.7)	16 (21.9)	0.704
Duration of hospitalization, days, median (IQR)	17.0 (13.5–27.0)	17.5 (13.75–27.25)	18.5 (13.75–27.0)	0.383
Total hospitalization expenses, ¥, median (IQR)	37,200.17 (21,000.59–67,381.93)	53,535.32 (32,783.81–72,962.02)	47,659.78 (24,210.15–69,156.10)	0.145

**Table 2.** Comparative analysis of hospitalization and follow-up outcomes between the two groups. GCS, Glasgow Coma Scale; HE, hematoma evacuation; mRS, modified Rankin Scale; IQR, interquartile range; a, missing data.

Variables	$\beta$ value	OR	95% CI	P-value	Score
Blend sign	1.946	7.003	2.118–23.161	0.001	2
Irregular shape	−1.447	0.235	0.067–0.821	0.023	−1
Two drainage tubes	3.355	28.643	1.872–438.181	0.016	3
Diabetes	−2.553	0.078	0.006–0.948	0.045	−3
Hematoma edge linked to ventricle	−1.931	0.145	0.032–0.659	0.012	−2
Constant	2.567	13.021			

**Table 3.** Results of multivariate logistic regression and assigned score for the risk of HE rates  $\geq 70\%$ . OR, odds ratio; CI, confidence interval; HE, hematoma evacuation.

to −1 have a lower likelihood of achieving HE rates  $\geq 70\%$ , whereas those with scores from 0 to 5 demonstrate an increased probability. One case was presented in Supplementary Figure S2.

We generate calibration plots, which exhibits good consistency between the model's predicted probabilities of HE rates  $\geq 70\%$  and actual observed outcomes (Fig. 2). Through the application of bootstrap internal validation, the cohort underwent 1000 iterations of resampling to derive ROC curves for various datasets. The mean AUC value for Model-logit was 0.819 (95% CI 0.763–0.903), the Model-score exhibited a mean AUC value of 0.823 (95% CI 0.742–0.903) (Fig. 3). These findings suggest that both models demonstrate robust stability. DCA demonstrated robust clinical utility for both predictive models in identifying HE rates  $\geq 70\%$ , with significant net benefit observed across a broad spectrum of decision thresholds (10–82%) (Fig. 3).

## Discussion

We conducted comprehensive analyses of clinical and radiographic characteristics in a cohort of supratentorial sICH patients undergoing stereotactic hematoma aspiration and catheter drainage, systematically identifying variables predictive of HE rates  $\geq 70\%$ . Leveraging these predictors, we developed a predictive model, rigorously assessing its discriminative performance via ROC analysis and calibration plots. The model's reproducibility and generalizability were further verified through internal validation employing 1000 bootstrap resampling iterations. In the MISTIE III trial, minimally invasive surgery with thrombolysis for moderate to severe sICH did not improve 1-year functional outcomes, but exploratory analyses of HE showed that reducing residual hematoma volume to less than 15 mL or HE greater than 70%, favorable functional results may be obtained by 1 year<sup>11</sup>. The research team further assessed the surgical outcomes of the MISTIE trial, establishing that after adjusting for baseline disease severity, achieving an end-of-treatment hematoma volume of  $\leq 15$  mL or a volumetric reduction of  $\geq 70\%$  was associated with improved functional independence (OR 1.06, 95% CI 1.02–1.10,  $P=0.002$ ), each 1 mL hematoma volume reduction translated to a 6% incremental probability of attaining functional independence (mRS 0–3)<sup>13</sup>. Therefore, we chose a 70% threshold for HE to conduct a correlation analysis. Patients with a HE rates  $\geq 70\%$  had shorter durations of drainage tube placement and a trend towards lower hospitalization costs (37,200.17 ¥ vs 53,535.32 ¥). However, regarding prognosis, similar to the results of the MISTIE trial, there were no significant differences in the mRS scores between the two patient groups at discharge and during follow-up. This may be attributed to the complex pathophysiology of sICH. Notably, this multicenter study pioneers the investigation of HE rates predictors following stereotactic hematoma aspiration and catheter drainage for sICH. By developing and validating a novel scoring system, our findings provide clinicians with an evidence-based tool for preoperative risk assessment and individualized treatment planning.

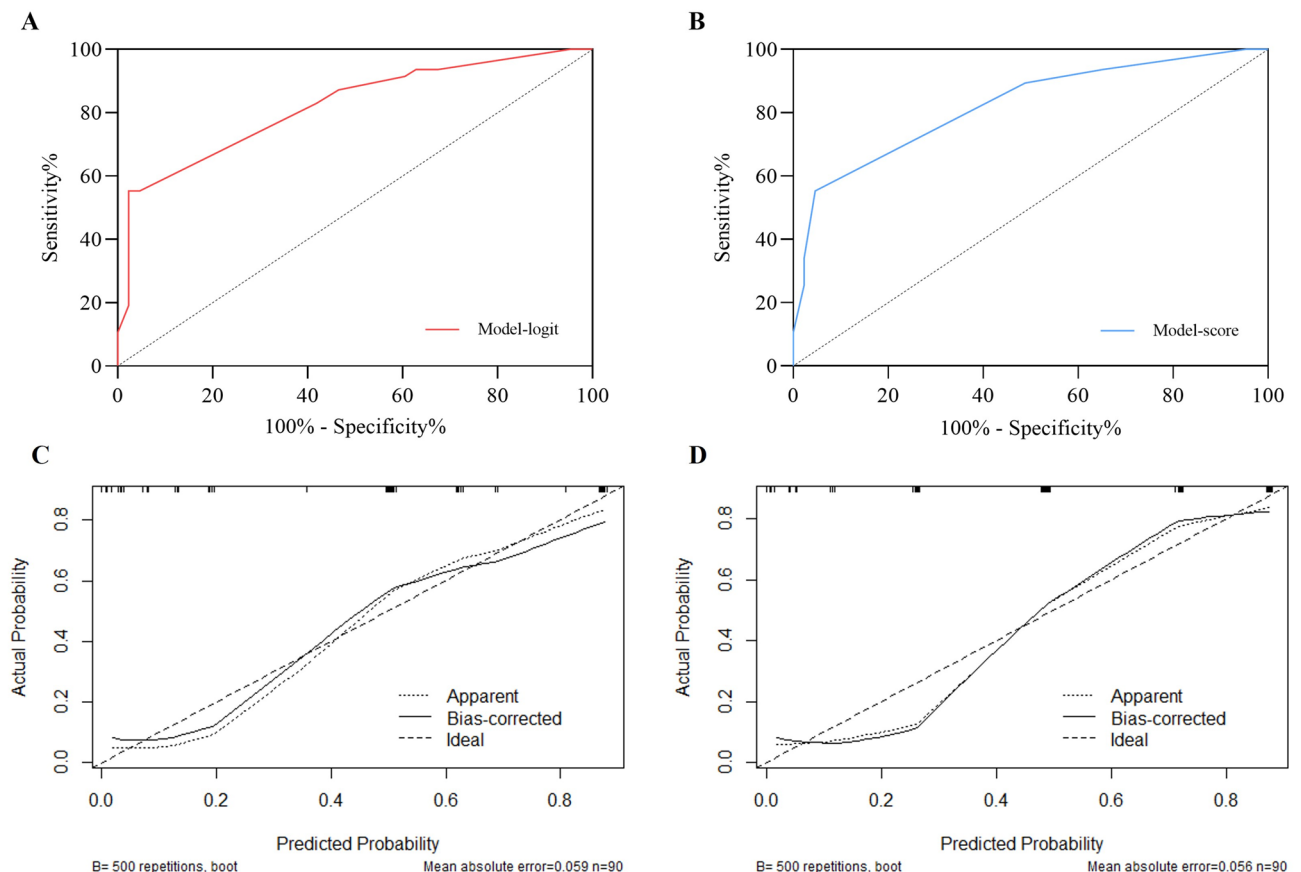


**Fig. 2.** (A) ROC curve analysis for the Model-logit, AUC was 0.820 (95% CI 0.733–0.906), with a cutoff value of 0.275; (B) ROC curve analysis for the Model-score, AUC was 0.822 (95% CI 0.737–0.908), with a cutoff value of -0.5; (C) Calibration curve analysis for the Model-logit; (D) Calibration curve analysis for the Model-score. AUC, area under the curve; CI, Confidence interval; Model-logit, logistic model; Model-score, scoring model; ROC, receiver operating characteristic.

Previous scholarly investigations have demonstrated that the blend sign can serve as an indicator of active bleeding and reflect various stages of hematoma development<sup>23</sup>. Notably, the attenuation values observed on CT scans are intimately linked to the hemoglobin content within the hematoma<sup>30</sup>. In the initial phase of hemorrhage, red blood cells remain intact, resulting in a relatively low concentration of hemoglobin within the hematoma. Consequently, this manifests as low attenuation on CT images. Subsequently, as the red blood cells undergo lysis, hemoglobin is released, and the clot undergoes shrinkage, leading to the separation of serum<sup>31</sup>. This process significantly elevates the hemoglobin concentration, ultimately resulting in a high attenuation signal on CT. Consequently, a positive blend sign may suggest the presence of a mobile liquid hematoma, which is more amenable to drainage, thereby facilitating HE rates.

As an NCCT marker, the irregular shape of hematoma is associated with hematoma expansion<sup>25</sup>. This may reflect the multi-source bleeding in the hematoma, along the multi-path development. The irregular shape of the hematoma can hinder the uniform distribution of urokinase and efficient drainage, ultimately compromising HE rates. The large-size irregular hematoma may require multiple drainage tubes. In our study, two drainage tubes, perpendicular to the long axis and short axis of the hematoma, were retained to promote the clearance of the hematoma. However, this process increases brain tissue damage, leading to its limited clinical application. In our cohort, only 6.7% patients had two drainage tubes placed. The studies by Wang T et al. have not found that the number of catheters can affect hematoma evacuation<sup>32</sup>. Therefore, the effectiveness needs to be further explored. Remarkably, our investigation has uncovered that the existence of a connection between the hematoma edge and the ventricle unexpectedly impedes HE rates, thus challenging the established clinical understanding. We offer a plausible hypothesis to explain this observation: the infiltration of cerebrospinal fluid into the hematoma cavity potentially dilutes the concentration of urokinase, subsequently limiting the dissolution of blood clots and ultimately compromising the efficiency of HE rates. In clinical practice, urokinase is often used to dissolve blood clots and transform solid hematoma into liquid hematoma. Studies have shown that urokinase can be used as a safe and effective alternative to alteplase<sup>33</sup>, but the optimal dose of urokinase remains uncertain. In this study, 81.1% patients received urokinase in combination. However, subgroup analysis showed no significant difference in HE rates between patients with and without urokinase. Furthermore, the dosage of urokinase in this study

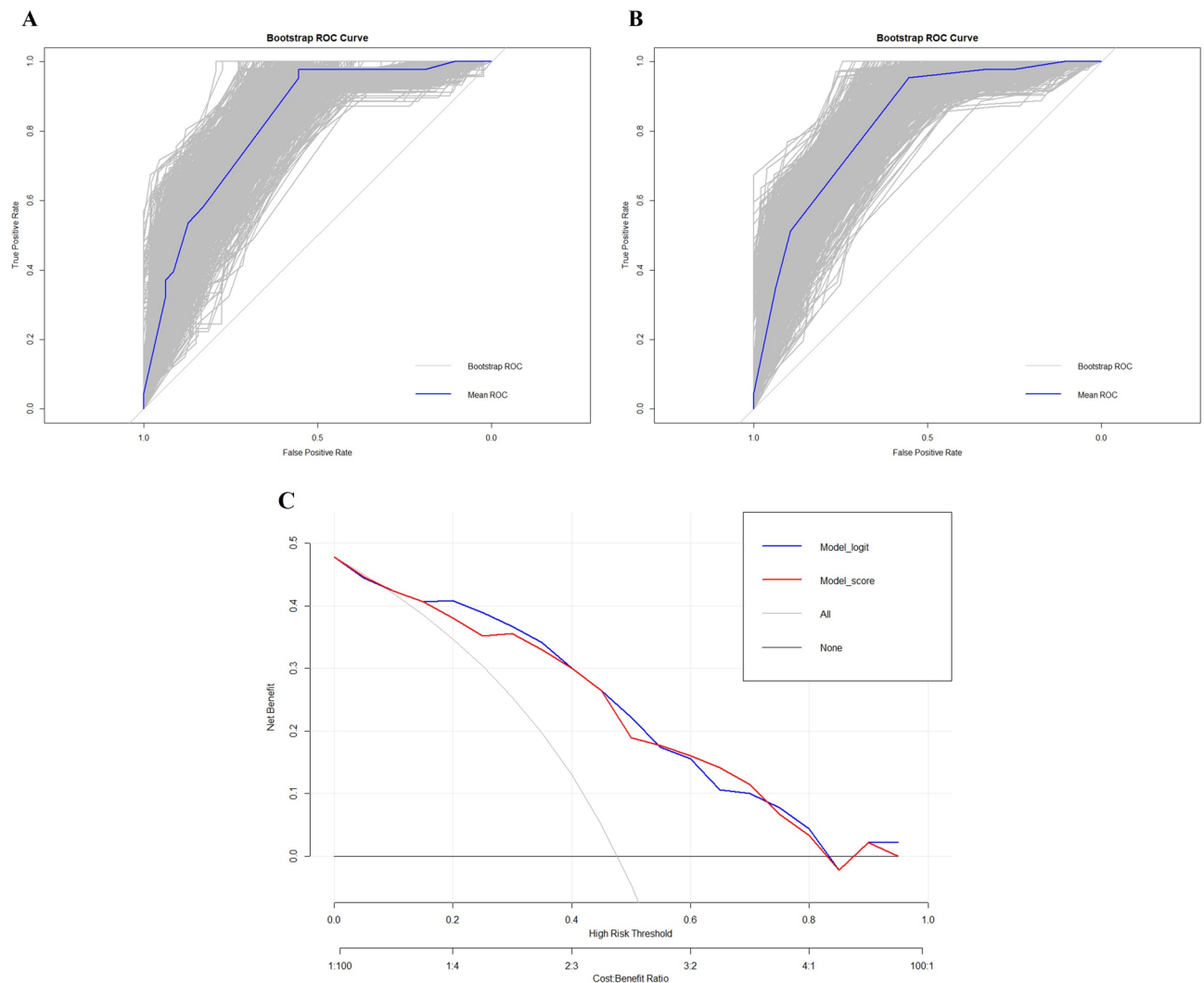


**Fig. 3.** (A) Bootstrap internal validation in Model-logit, with the mean AUC 0.819 (95% CI 0.736–0.903); (B) Bootstrap internal validation in Model-score, with the mean AUC 0.823 (95% CI 0.742–0.903). (C) Decision curve analysis of the model-logit (blue) and the model-score (red). The decision curve shows that if the threshold probability of an individual is 10–82%, using this model to predict HE rates  $\geq 70\%$  is better. AUC, area under the curve; CI, Confidence interval; HE, hematoma evacuation, Model-logit, logistic model; Model-score, scoring model.

ranged from 5000 IU to 50,000 IU. Future studies should aim to develop standardized urokinase administration protocols and verify the effect of urokinase on HE rates, as well as ascertain the optimal dosage.

Diabetes is associated with increased risk of sICH, which may promote vascular wall damage in the brain and form atherosclerosis and other vascular lesions through oxidative stress and inflammatory reaction<sup>34</sup>. About 26% of the hemorrhagic stroke were accompanied by diabetes<sup>35</sup>. In our study, with the history of diabetes was not conducive to hematoma evacuation. At present, there are few related literatures, and the specific mechanism still needs to be further explored. Kim JH et al. hypothesized that the blood viscosity of patients with diabetes is high<sup>36</sup>. And according to the previous research results: in diabetes, coagulation and plasminogen activator inhibitor levels are increased, while fibrinolytic activity is decreased, it is speculated that blood clots in the brain of diabetic patients are not easily dissolved and excreted<sup>37</sup>.

Drawing upon the aforementioned conclusions, we have developed a scoring predictive model, which is convenient and accurate. Within the framework of the Model-score, patients scoring of 0 to 5 demonstrate a significantly elevated likelihood of achieving HE rates of 70% or higher.

There are still some potential limitations in our study. Firstly, although it comes from a prospective, multicenter cerebral hemorrhage registry database, the sample size is small, which may affect the conclusion of the study and its universality. Secondly, the predictive model employed in this study has yet to undergo external validation, however, we have implemented internal validation through bootstrap resampling, and the model has exhibited robust stability. Thirdly, the heterogeneity in follow-up intervals across patients may confound the prognostic evaluation of HE rates  $\geq 70\%$ , necessitating future investigations with standardized follow-up



protocols to validate these associations. Finally, our analysis was intentionally restricted to patients undergoing stereotactic aspiration and catheter drainage to reduce procedural variability. It excludes conservatively managed patients and those receiving alternative surgical interventions. This limits the generalizability of our findings to broader clinical scenarios. Future multicenter studies should compare HE rates between stereotactic aspiration with catheter drainage and alternative surgical approaches (e.g., craniotomy, endoscopic evacuation) across hematoma volumes. Integrating machine learning-based predictive models could further optimize surgical decision-making and outcome stratification.

## Conclusion

Our findings suggest that for sICH patients undergoing stereotactic aspiration and catheter drainage, positive preoperative NCCT blend sign and with two drainage tubes can promote hematoma evacuation, while diabetes history, irregular shape of hematoma, and connection between the edge of hematoma and cerebral ventricle are not conducive to hematoma evacuation. The predictive model for HE rates possesses the advantages of simplicity and convenience, providing clinicians with a reference for enhancing the efficiency of minimally invasive surgery procedures.

## Data availability

Data are available from the corresponding author on reasonable request.

Received: 14 January 2025; Accepted: 8 May 2025

Published online: 22 May 2025

## References

- Qureshi, A. I., Mendelow, A. D. & Hanley, D. F. Intracerebral haemorrhage. *Lancet* **373**(9675), 1632–1644 (2009).
- Al-Shahi Salman, R., Labovitz, D. L. & Stapf, C. Spontaneous intracerebral haemorrhage. *BMJ* **339**, b2586. <https://doi.org/10.1136/bmj.b2586> (2009).
- Kim, J. Y. & Bae, H. J. Spontaneous intracerebral hemorrhage: Management. *J. Stroke* **19**(1), 28–39. <https://doi.org/10.5853/jos.2016.01935> (2017).
- Tsai, C. F., Thomas, B. & Sudlow, C. L. Epidemiology of stroke and its subtypes in Chinese vs white populations: A systematic review. *Neurology* **81**(3), 264–272 (2013).
- Diringer, M. N. Intracerebral hemorrhage: pathophysiology and management. *Crit Care Med.* **21**(10), 1591–1603 (1993).
- van Etten, E. S. et al. Trigger factors for spontaneous intracerebral hemorrhage: A case-crossover study. *Stroke* **53**(5), 1692–1699 (2022).
- Rzepliński, R. et al. Mechanism of spontaneous intracerebral hemorrhage formation: An anatomical specimens-based study. *Stroke* **53**(11), 3474–3480 (2022).
- Wan, J., Ren, H. & Wang, J. Iron toxicity, lipid peroxidation and ferroptosis after intracerebral haemorrhage. *Stroke Vasc Neurol.* **4**(2), 93–95 (2019).
- Hemphill, J. C. 3rd. et al. Guidelines for the management of spontaneous intracerebral hemorrhage: A guideline for healthcare professionals from the American Heart Association/American Stroke Association. *Stroke* **46**(7), 2032–2060 (2015).
- de Oliveira Manoel, A. L. Surgery for spontaneous intracerebral hemorrhage. *Crit Care* **24**(1), 45 (2020).
- Hanley, D. F. et al. Efficacy and safety of minimally invasive surgery with thrombolysis in intracerebral haemorrhage evacuation (MISTIE III): A randomised, controlled, open-label, blinded endpoint phase 3 trial. *Lancet* **393**(10175), 1021–1032 (2019).
- Pradilla, G. et al. Trial of early minimally invasive removal of intracerebral hemorrhage. *N. Engl. J. Med.* **390**(14), 1277–1289 (2024).
- Awad, I. A. et al. Surgical performance determines functional outcome benefit in the minimally invasive surgery plus recombinant tissue plasminogen activator for intracerebral hemorrhage evacuation (MISTIE) Procedure. *Neurosurgery* **84**(6), 1157–1168 (2019).
- Guo, W. et al. Comparison of endoscopic evacuation, stereotactic aspiration, and craniotomy for treatment of basal ganglia hemorrhage. *J. Neurointerv. Surg.* **12**(1), 55–61 (2020).
- Wang, J. W. et al. Stereotactic aspiration versus craniotomy for primary intracerebral hemorrhage: A meta-analysis of randomized controlled trials. *PLoS ONE* **9**(9), e107614 (2014).
- Kumar, S. et al. Comparison of craniotomy and stereotactic aspiration plus thrombolysis in isolated capsulo-ganglionic hematoma: A retrospective analyses. *Neurol. India* **70**(2), 535–542 (2022).
- Lin, F. et al. Early deterioration and long-term prognosis of patients with intracerebral hemorrhage along with hematoma volume more than 20 ml: Who needs surgery?. *Front Neurol.* **12**, 789060 (2022).
- Feng, H., Wang, X., Wang, W. & Zhao, X. Risk factors and a prediction model for the prognosis of intracerebral hemorrhage using cerebral microhemorrhage and clinical factors. *Front Neurol.* **14**, 1268627 (2023).
- Urday, S. et al. Targeting secondary injury in intracerebral haemorrhage—perihematomal oedema. *Nat. Rev. Neurol.* **11**(2), 111–122 (2015).
- Li, Q. et al. Black hole sign: Novel imaging marker that predicts hematoma growth in patients with intracerebral hemorrhage. *Stroke* **47**(7), 1777–1781 (2016).
- Li, Q. et al. Island sign: An imaging predictor for early hematoma expansion and poor outcome in patients with intracerebral hemorrhage. *Stroke* **48**(11), 3019–3025 (2017).
- Yu, Z. et al. Significance of satellite sign and spot sign in predicting hematoma expansion in spontaneous intracerebral hemorrhage. *Clin. Neurol. Neurosurg.* **162**, 67–71 (2017).
- Li, Q. et al. Blend sign on computed tomography: Novel and reliable predictor for early hematoma growth in patients with intracerebral hemorrhage. *Stroke* **46**(8), 2119–2123 (2015).
- Sato, S. et al. Determinants and prognostic significance of hematoma sedimentation levels in acute intracerebral hemorrhage. *Cerebrovasc. Dis.* **41**(1–2), 80–86 (2016).
- Barras, C. D. et al. Density and shape as CT predictors of intracerebral hemorrhage growth. *Stroke* **40**(4), 1325–1331 (2009).
- Mendelow, A. D. et al. Early surgery versus initial conservative treatment in patients with spontaneous supratentorial intracerebral haematomas in the International Surgical Trial in Intracerebral Haemorrhage (STICH): a randomised trial. *Lancet* **365**(9457), 387–397 (2005).
- Demchuk, A. M. et al. Prediction of haematoma growth and outcome in patients with intracerebral haemorrhage using the CT-angiography spot sign (PREDICT): a prospective observational study. *Lancet Neurol.* **11**(4), 307–314 (2012).

28. Malinova, V., Schlegel, A., Rohde, V. & Mielke, D. Catheter placement for lysis of spontaneous intracerebral hematomas: does a catheter position in the core of the hematoma allow more effective and faster hematoma lysis?. *Neurosurg. Rev.* **40**(3), 397–402 (2017).
29. Polster, S. P. et al. Thrombolysis for evacuation of intracerebral and intraventricular hemorrhage: A guide to surgical protocols with practical lessons learned from the MISTIE and CLEAR Trials. *Oper. Neurosurg. (Hagerstown)*. **20**(1), 98–108 (2020).
30. Nowinski, W. L. et al. Characterization of intraventricular and intracerebral hematomas in non-contrast CT. *Neuroradiol. J.* **27**(3), 299–315 (2014).
31. New, P. F. & Aronow, S. Attenuation measurements of whole blood and blood fractions in computed tomography. *Radiology* **121**(3 Pt. 1), 635–640 (1976).
32. Wang, T. et al. Factors affecting the evacuation rate of intracerebral hemorrhage in basal ganglia treated by minimally invasive craniopuncture. *Clin. Neurol. Neurosurg.* **134**, 104–109 (2015).
33. Zhang, X. et al. Stereotactic aspiration for hypertensive intracerebral haemorrhage in a Chinese population: A retrospective cohort study. *Stroke Vasc. Neurol.* **4**(1), 14–21 (2019).
34. Saliba, W. et al. Association of diabetes and glycated hemoglobin with the risk of intracerebral hemorrhage: A population-based cohort study. *Diabetes Care* **42**(4), 682–688 (2019).
35. Lau, L. H., Lew, J., Borschmann, K., Thijs, V. & Ekinici, E. I. Prevalence of diabetes and its effects on stroke outcomes: A meta-analysis and literature review. *J. Diabetes Investig.* **10**(3), 780–792 (2019).
36. Kim, J. H. et al. Clinical and radiographic factors involved in achieving a hematoma evacuation rate of more than 70% through minimally invasive catheter drainage for spontaneous intracerebral hemorrhage. *J. Clin. Neurosci.* **92**, 103–109 (2021).
37. Karapanayiotides, T., Piechowski-Jozwiak, B., van Melle, G., Bogousslavsky, J. & Devuyst, G. Stroke patterns, etiology, and prognosis in patients with diabetes mellitus. *Neurology* **62**(9), 1558–1562 (2004).

## Author contributions

All persons who meet authorship criteria are listed as authors. WHF and DZK proposed research concepts and designs, provided support, and supervised the study. DZK, WHF, and HCSG obtained the funding. XQL and KMS prepared the draft manuscript and coordinated its finalization. XQL and LYZ performed statistical analyses; XQL and FXL drew and prepared the tables and figures. ZYG, QH, YZ, KBL and HCSG gathered pertinent data, performed database management and data cleaning. YXL, FXL, and XGL revised the manuscript. All authors have seen and approved the final manuscript.

## Funding

This work was funded by the Fujian Provincial Medical Center for Neurological Diseases, under the grant for the “Double High” Construction Project in Neurosurgery Research (2023YSJYX-PD-4, 2023YSJYX-YL-6), Fujian Provincial Health and Wellness Social Science Program (2022RKA005), and the Fujian Provincial Health Commission (2022ZD01003).

## Declarations

## Competing interests

The authors declare no competing interests.

## Ethics approval

This study was approved by the Ethics Committee of the First Affiliated Hospital of Fujian Medical University (Ethical Approval Number: MRCTA, ECFAH of FMU [2018] 082-1).

## Additional information

**Supplementary Information** The online version contains supplementary material available at <https://doi.org/10.1038/s41598-025-01754-0>.

**Correspondence** and requests for materials should be addressed to D.K. or W.F.

**Reprints and permissions information** is available at [www.nature.com/reprints](http://www.nature.com/reprints).

**Publisher's note** Springer Nature remains neutral with regard to jurisdictional claims in published maps and institutional affiliations.

**Open Access** This article is licensed under a Creative Commons Attribution-NonCommercial-NoDerivatives 4.0 International License, which permits any non-commercial use, sharing, distribution and reproduction in any medium or format, as long as you give appropriate credit to the original author(s) and the source, provide a link to the Creative Commons licence, and indicate if you modified the licensed material. You do not have permission under this licence to share adapted material derived from this article or parts of it. The images or other third party material in this article are included in the article's Creative Commons licence, unless indicated otherwise in a credit line to the material. If material is not included in the article's Creative Commons licence and your intended use is not permitted by statutory regulation or exceeds the permitted use, you will need to obtain permission directly from the copyright holder. To view a copy of this licence, visit <http://creativecommons.org/licenses/by-nc-nd/4.0/>.

© The Author(s) 2025